Molecular BioSystems

Accepted Manuscript

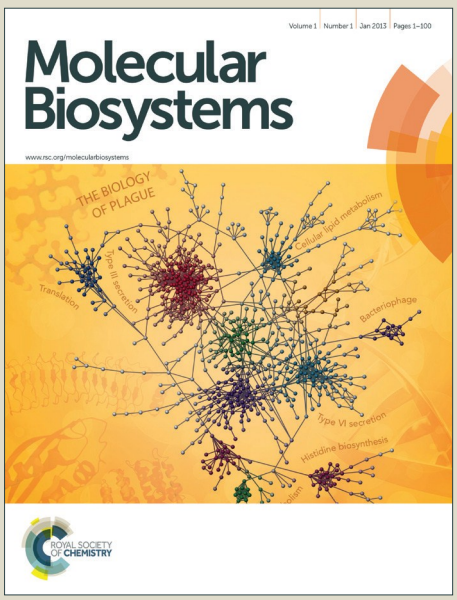

ROYAL SOCIETY OF CHEMISTRY

www.rsc.org/molecularbiosystems

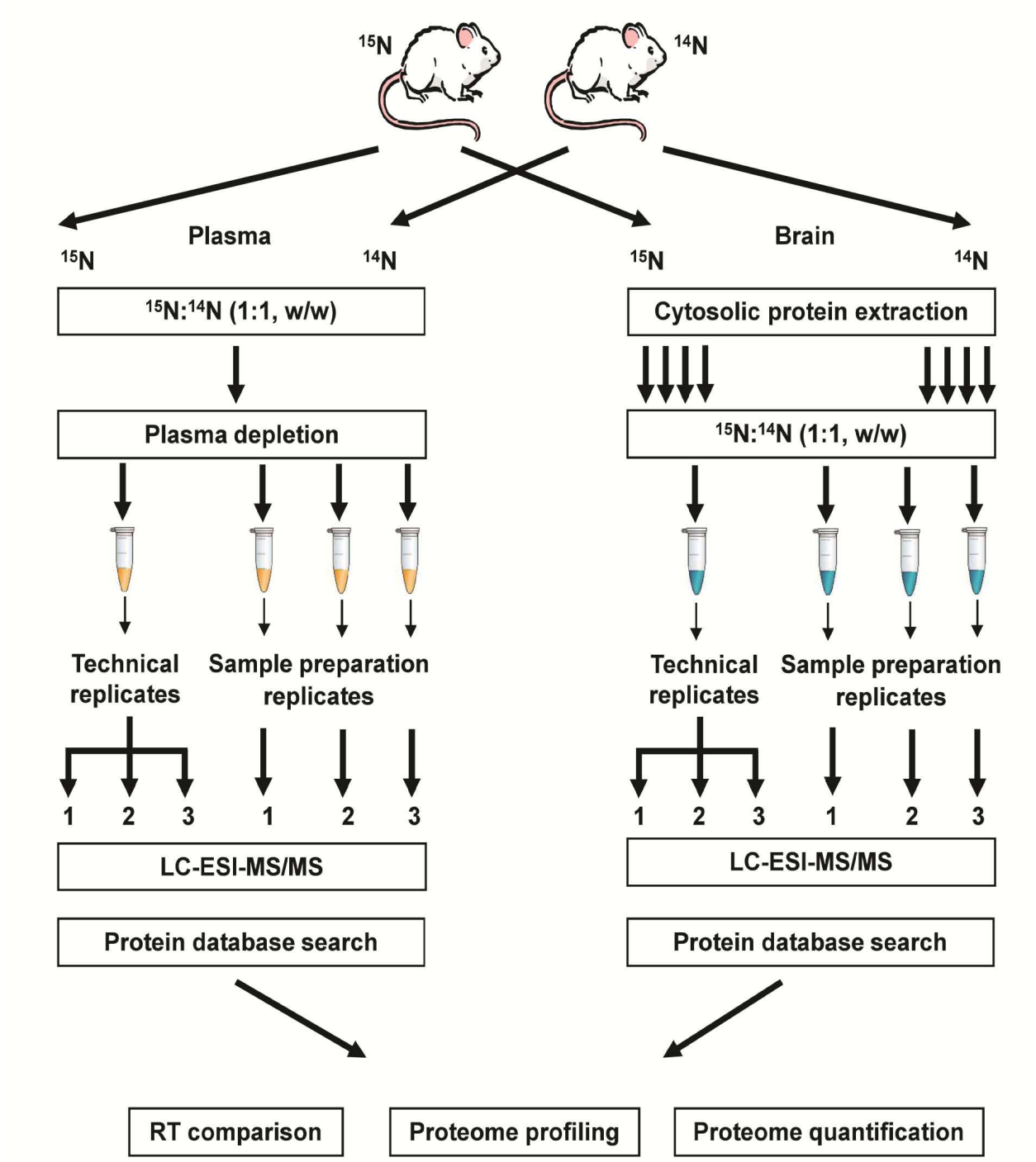

Repeatability of the ^{15}N metabolic labeling workflow for quantitative proteomics in mouse plasma and brain specimens.

Variability assessment of ^{15}N metabolic labeling-based proteomics workflow in mouse brain and plasma

Michaela D. Filiou, Magdalena Soukupova, Christiane Rewerts, Christian Webhofer[1], Chris W. Turck, Giuseppina Maccarrone*

Max Planck Institute of Psychiatry, Kraepelinstr. 2, 80804, Munich, Germany

[1]Current address: Sandoz Biopharmaceuticals, Keltenring 1+3, 82041 Oberhaching, Germany

*Address for correspondence

Giuseppina Maccarrone, PhD

Max Planck Institute of Psychiatry

Kraepelinstr. 2

80804 Munich, Germany

Tel: +49 89 30622 211

Fax: +49 89 30622 610

Email: maccarrone@mpipsykl.mpg.de

Abbreviations: RT: retention time

Keywords: ^{15}N metabolic labeling, mice, quantitative proteomics, technical repeatability

Abstract

^{15}N metabolic labeling-based quantitative proteomics is used for the identification of disease- and phenotype-related alterations in live organisms. The variability of ^{15}N metabolic labeling proteomics workflows has been assessed in plants and bacteria. However, no study has addressed this topic in mice. We have investigated the repeatability of a quantitative *in vivo* ^{15}N metabolic labeling proteomics workflow in mice by assessing LC variability, peptide and protein profiling characteristics and overall $^{15}N/^{14}N$ protein quantification accuracy in technical replicates of plasma and brain specimens. We furthermore examined how sample preparation affects these parameters in brain and plasma. We found that specimen type (i.e. plasma or brain) influences the variability of the ^{15}N metabolic labeling workflow in an LC-independent manner.

Introduction

In vivo ^{15}N metabolic labeling is a valuable tool for quantitative proteomics and hypothesis-free identification of molecular biosignatures in model organisms and has been successfully applied to mouse models of cancer and psychiatric disorders [1-7]. The stable isotope metabolic labeling method represents the gold standard for the quantitative proteomics analysis by mass spectrometry. The main advantage of this method is that the labeled and unlabeled samples are mixed at early steps of the sample preparation workflow, thus minimizing experimental bias during sample handling.

To ensure an optimal cost- and time-effective application of the ^{15}N metabolic labeling quantification workflow, the contributing factors accounting for technical and biological variability need to be examined. To date, technical variability of ^{15}N labeling workflows has been investigated in *Arabidopsis thaliana* and *Escherichia coli* [8-11]. However, no study has addressed the technical and sample preparation variabilities of ^{15}N metabolic labeling workflows in mice. We have addressed biological variation in our previous mouse studies [1, 2]. Here, technical variability was assessed both in brain and plasma by mixing plasma and brain specimens from ^{15}N-labeled and unlabeled 56 days old male mice, respectively, at a 1:1 ratio and measuring the $^{15}N/^{14}N$ plasma and the $^{15}N/^{14}N$ brain specimens three times each by nanoLC-ESI-MS/MS (technical replicates of plasma and brain specimens). The contribution of sample preparation to overall method variability was also assessed by measuring three different plasma specimens derived from the same $^{15}N/^{14}N$ depleted protein fraction and three different brain specimens derived from the same $^{15}N/^{14}N$ protein extract. Each specimen was processed independently for MS analysis (sample preparation replicates in plasma and brain). Sample preparation included

all the experimental steps that follow protein depletion and protein extraction of plasma and brain, respectively. Protein depletion and protein extraction were not considered as this step of the sample preparation workflow may vary according to the study objectives. The variability of the following parameters was assessed: (i) LC retention times (RTs) of eluted peptides (ii) number and overlap of peptide and protein identifications (iii) identified peptides per protein and sequence coverage distribution (iv) $^{15}N/^{14}N$ protein quantification ratios. The experimental set up is shown in **Fig. 1**.

Materials and methods

Animals

The animal experiments were approved by local authorities and conducted according to current regulations for animal experimentation in Germany and the European Union (European Communities Council Directive 86/609/EEC). Mice were metabolically labeled *in vivo* with a ^{15}N-labeled bacteria-based diet starting *in utero* and for 56 days *post partum*, achieving >90% ^{15}N incorporation both in plasma and brain [7]. Unlabeled mice received the same bacteria-based diet with natural ^{15}N abundance.

Proteomics sample preparation

Brain tissue was acquired after perfusion with 0.9% saline. Blood from the same mouse was sampled prior to perfusion and plasma was collected by centrifugation for 10min at 1300g and 4°C. For plasma proteome analysis, equal total protein amounts of ^{15}N-labeled and unlabeled plasma (400µg each) were combined and the three highly abundant proteins albumin, IgG and transferrin were depleted from the combined $^{15}N/^{14}N$ mixture

by the Multiple Affinity Removal Spin cartridge mouse 3 (MARS3, Agilent Technologies, Santa Clara, CA) following the manufacturer's instructions. From the depleted plasma, three aliquots (40µg each) were generated. Protein content was estimated by Bradford assay (BioRad, Hercules, CA) (sample preparation replicates 1, 2, 3). For brain proteome analysis, the cytosolic fractions from a ^{15}N-labeled and an unlabeled brain were enriched according to [12]. From each cytosolic fraction, three aliquots (0.2ml each) were generated. Protein content was determined for each aliquot by independent Bradford assays (BioRad). Equal protein amounts of ^{15}N-labeled and unlabeled aliquots (25µg each) were then combined to generate three ^{15}N/^{14}N cytosolic protein extracts (sample preparation replicates 1, 2, 3). The three ^{15}N/^{14}N plasma specimens and three brain extracts were loaded onto the same one dimensional SDS-PAGE. After electrophoresis, the proteins were stained by Coomassie Brilliant (BioRad) and each gel lane was cut into 24 slices. In-gel digestion and peptide extraction were performed as previously described [7]. Each extracted peptide fraction was filtered with Costar SpinX tube filters (0.22µm, Sigma-Aldrich, Munich, Germany). The filtered peptide extracts were then pooled in sets of four, resulting in six fractions per lane.

LC-ESI MS/MS analysis

Nano LC-ESI-MS/MS analysis of the peptide fractions was carried out with an LTQ-Orbitrap mass spectrometer (Thermo Fisher Scientific, Bremen, Germany) coupled online to a HPLC-2D system (Eksigent, Dublin, CA) *via* a nanoelectrospray ion source (Thermo Fisher Scientific). The peptide fractions were dissolved in 0.1% formic acid aqueous solution (Merck, Darmstadt, Germany) and loaded onto an in-house packed

fused silica 5µm nano RP-C18 (Maisch, Monheim, Germany) column (0.075mm x 20cm). The nano column was washed with 0.1% formic acid for 10min and eluted with a gradient of 95% acetonitrile/0.1% formic acid from 2% to 10% in 2min, from 10 to 40% in 93min at a flow rate of 200nl/min. The mass spectrometer was operated in positive ion mode and data-dependent acquisition mode at ion spray voltage 1.7 kV. Full scans were recorded in the Orbitrap mass analyzer at a mass range of m/z 380–1,600 at resolution of 60,000 (m/z 400) in profile mode. The MS/MS analysis of the five most intense peptide ions for each scan was recorded in the LTQ mass analyzer in centroid mode. Additional MS parameters were as previously described in [13] and are summarized in electronic supplementary information (**ESI**). One plasma and one brain gel lane were measured three times each to generate the corresponding plasma and brain technical replicates 1, 2, 3. All experiments were performed by the same operator.

Proteomics data analysis

MS raw data were searched against a ^{14}N and ^{15}N mouse decoy database (UniProt mouse_v. 11.07.2012) generated by Sequest v. 28 (Thermo Fischer Scientific, San Jose, CA). The protein database search was performed using Bioworks v. 3.3.1 (Thermo Fischer Scientific, San Jose, CA). Database searches were carried out by using either unlabeled amino acids or ^{15}N-labeled amino acids (^{15}N enriched amino acids option enabled). Search parameters were as previously described [14]. Briefly, precursor and fragment ion mass accuracy were set 10ppm and 0.8Da, respectively. Methionine oxidation and cysteine carboxyamidomethylation were included as variable and static modifications, respectively. Two tryptic missed cleavages were allowed. In addition, a

variable modification of -1Da for lysine and arginine residues was assigned to take into consideration the precursor mass shift from the ^{15}N monoisotopic to the most intensive ^{15}N-labeled isotopologue triggered for MS/MS [15]. The ^{14}N and ^{15}N peptides were filtered at false discovery rate of 1% by PeptideProphet [16]. Using the Trans-Proteomic Pipeline (TPP), ^{14}N and ^{15}N proteins were combined and grouped by iProphet [17].

^{15}N incorporation in plasma and brain was calculated by Atomizer [18]. Relative $^{15}N/^{14}N$ protein quantification was performed by ProRata software (v1.0) using default parameters [19]. Log_2 ($^{15}N/^{14}N$) ratios were assigned to protein groups and proteins quantified by at least two peptides were accepted. The log_2 ratios of overlapping proteins across brain or plasma replicate pairs were compared [19]. MS raw and $^{15}N/^{14}N$ quantification data are available upon request.

Peptide RTs from the individual fractions were combined per replicate and overlapping peptide sequences across all replicates were selected by an in-house developed script written in R. For each replicate pair in plasma or brain the overlapping unlabeled peptides RTs were compared. Only protein groups identified with at least two unique peptides per replicate were considered. The percentage of the overlapping proteins and peptides across the three replicates was calculated by BioVenn [20].

Results and Discussion

We first evaluated LC variability by comparing peptide RTs across brain and plasma technical replicates. Peptide RTs were highly reproducible, with an average RT correlation coefficient of 0.96 for plasma and 0.98 for brain. RT correlation coefficients for each technical replicate pair are shown in **Fig. S1A**, **ESI**. We then investigated the

repeatability of peptide and protein profiling characteristics. In plasma, 2802 unique peptides and 325 unique proteins were identified in all three technical replicates. In brain, 11728 unique peptides and 2419 unique proteins were identified in all technical replicates. The unique identified proteins per technical replicate were grouped and the resulted group numbers are shown in **Table 1**. For plasma, the overlap of identified peptides and protein groups in all three replicates is 60.26% and 69.65%, respectively. The corresponding overlaps for brain were lower 51.04% and 65.46% for identified peptides and protein groups, respectively (**Fig. S1B**, **ESI**). Furthermore, the distribution profiles of peptides per protein were similar across technical replicates both in brain and plasma. Notably, a shift towards protein groups identified by fewer peptides was observed for brain specimens. Almost 50% of the brain proteins and only 35% of the plasma proteins were identified by 3-8 peptides. In addition, 1% of brain proteins as opposed to up to 10% plasma proteins were identified with >40 peptides. These variations may be attributed to the presence of several very high abundant proteins in plasma [21]. The distribution of protein sequence coverage (%) was comparable across technical replicates both in plasma and brain (**Fig. 2A**).

Besides peptide and protein profiling characterization we evaluated the overall variability of the ^{15}N metabolic labeling workflow by assessing the $\log_2(^{15}N/^{14}N)$ protein quantification ratios which constitute the workflow endpoint readout. We plotted the $\log_2(^{15}N/^{14}N)$ ratios of the overlapping quantified protein groups in all three replicates per specimen type (i.e. plasma or brain) (**Fig. S1C**, **ESI**). The average correlation coefficients for $\log_2(^{15}N/^{14}N)$ ratios for technical replicate pairs in plasma and brain were 0.91 and 0.78, respectively. Taken together, the comparison of the plasma and brain data revealed

that specimen type exerts an effect on the ^{15}N quantification workflow precision as evidenced by (i) decreased peptide and protein group identification overlap (ii) increased protein group identifications with a lower peptide number and (iii) an overall increased variability of $\log_2(^{15}N/^{14}N)$ ratios in brain compared to plasma. LC performance and sequence coverage (%) distribution appeared to remain unaffected by specimen type.

We then examined how sample preparation affects relative protein quantification variability in mouse plasma and brain specimens. We compared the three plasma sample preparation replicates and the three brain sample preparation replicates that were independently processed for MS analysis. The average RT correlation coefficient for plasma and brain sample preparation replicates was 0.93 and 0.95, respectively (**Fig. S1D**, **ESI**) compared to 0.96 for plasma and 0.98 for brain technical replicates, indicating a high LC precision, irrespective of the specimen studied. We identified 3270 and 12114 unique peptides corresponding to 340 and 2313 unique proteins in all three plasma and brain sample preparation replicates, respectively. The unique identified proteins per plasma and brain sample replicate were grouped and the resulting group numbers are shown in **Table 1**. Peptide and protein group overlap across all brain sample preparation replicates decreased dramatically compared to brain technical replicates with 30.68% and 50.18% overlaps, respectively. In plasma, peptide and protein overlap across all three sample preparation replicates was lower compared to plasma technical replicates with 41.39% and 60.75% overlaps, respectively (**Fig. S1E**, **ESI**). The distribution of identified peptide number per protein in plasma and brain sample preparation replicates was comparable to plasma and brain technical replicates respectively, with only a slight increase in variability across replicates in protein groups identified by 3-8 peptides.

However, when comparing the sequence coverage (%) distribution we observed an overall increased variability in plasma and brain sample preparation replicates. In plasma the variability was most prominent in protein groups with sequence coverage ≤20%; in brain the variability increased in protein groups with sequence coverage of <10% (**Fig. 2B**). Low sequence coverage does not necessarily imply low abundance but it may also depend on protein length and digestion pattern [22]. The average $\log_2(^{15}N/^{14}N)$ ratio correlation coefficient for plasma and brain is 0.84 and 0.76, respectively, and both are slightly lower than those for brain and for plasma technical replicates (**Fig. S1F, ESI**). Taken together, we show that sample preparation variability resulted in (i) decreased peptide and protein group identification overlaps (ii) increased variability in sequence coverage (%) distribution (iii) increased variability of $\log_2(^{15}N/^{14}N)$ ratios markedly in brain sample preparation replicates compared to brain and plasma technical replicates.

The main goal of this study was to assess the ^{15}N quantification workflow as a whole, providing an estimate of the overall method variability rather than conducting an exhaustive evaluation of individual experimental steps. Previous studies have addressed the ^{15}N metabolic labeling workflow variability in *Arabidopsis thaliana* and have provided a comprehensive evaluation of experimental parameters, including $^{15}N/^{14}N$ mixing ratios and proteome coverage based on starting material [8], distribution of $\log_2(^{15}N/^{14}N)$ ratios [10] as well as the contribution of individual sample preparation steps to overall quantification variability [11]. Here, we focused for the first time on mouse plasma and brain specimens. We observed an effect of specimen type and sample preparation at the peptide/protein group identification overlap across replicates. The partial overlap of peptide/protein identifications in repeated measurements [22] is largely attributable to the stochastic nature

of mass spectrometry, but also constitutes a reproducibility indicator [23]. Both in technical and sample preparation replicates the identification overlap (%) was higher for protein groups compared to peptides, in line with data acquired from unlabeled material [23]. Both for brain and plasma proteome the overlap of both peptide and protein groups in sample preparation replicates is lower compared to technical replicates. This difference may be attributed to experimental errors throughout the multiple steps of the sample preparation (i.e. variability in protein content estimation, $^{15}N/^{14}N$ mixing ratios). The repeatability between sample preparation replicates is comparable to that of technical replicates in brain, suggesting that specimen type rather than sample preparation affects quantification variability in this experimental set up. In our workflow analysis we did not consider protein extraction variability which has been reported to contribute the most to sample preparation variability [24]. Our data show that specimen type is a main contributing factor for quantification variability as summarized in **Table 2**. RT repeatability was >0.94 in all cases, indicating that the robust performance of the LC analysis is independent of specimen type or sample preparation. The peptides included in the present study fulfill a series of requirements which are specific for the employed ^{15}N metabolic labeling workflow, such as identification by both ^{14}N and ^{15}N database searches and isotope cluster intensities with a S/N >2 for subsequent quantification with *ProRata*. Low S/N intensities as well as overlapping isotope clusters result in inaccurate protein quantifications and do not contribute to the assessment of technical variability (**Fig. 3**). As a result, a lower number of analyzed peptides/proteins is reported compared to proteome profiling studies of mouse plasma and brain using only unlabeled material. Interestingly, relative $^{15}N/^{14}N$ quantification revealed a number of protein abundance differences between the 15N-

labeled and the unlabeled fractions (**Fig. S2**, **ESI**). As we have reported earlier, these are caused by a ^{15}N isotope effect on the mouse plasma and brain proteomes 14, 25.

Conclusion

In conclusion, we assessed the variability of a quantitative proteomics workflow using ^{15}N metabolic labeling in mouse plasma and brain. We report that specimen type plays a major role in quantification variability, which should be accurately defined prior to experimental implementation. A higher quantification reproducibility can be reached by separating the isotope clusters and increasing the peptide signal to noise ratio (S/N). Furthermore, in-depth fractionation at the protein and peptide levels may considerably contribute to reducing the overlapping cluster isotopes. An optimization of the mass spectrometry method for the acquisition of high signal quality rather than high speed acquisition will improve the S/N intensities leading to a decrease of the quantification variability and to quantification of low abundant peptides. Our findings provide for the first time a workflow for assessing technical variability for quantitative proteomics experiments in mouse models that will allow acquisition of robust quantitative information to answer pertinent biological questions.

Acknowledgments

M.D.F. is supported by a grant from the *Deutsche Forschungsgemeinschaft* (FI 1895/1-1). This work was funded by a BMBF *QuantPro* grant and the *Max Planck Society*. The authors would like to thank Daniel Martins-de-Souza for fruitful discussions.

Conflict of interest statement

The authors declare no conflict of interest.

References

1. M. D. Filiou, Y. Zhang , L. Teplytska, S. Reckow, P. Gormanns, G. Maccarrone, E. Frank, M. S. Kessler, B. Hambsch, M. Nussbaumer, M. Bunck, T. Ludwig, A. Yassouridis, F. Holsboer, R. Landgraf and C. W. Turck, *Biol Psychiatry*, 2011, 70, 1074-1082.
2. M. D. Filiou, L. Teplytska, D. M. Otte, A. Zimmer and C. W. Turck, *J Psychiatr Res*, 2012, 46, 1359-1365.
3. E. L. Huttlin, X. Chen, G. A. Barrett-Wilt, A. D. Hegeman, R. B. Halberg, A. C. Harms, M. A. Newton, W. F. Dove and M. R. Sussman, *Proc Natl Acad Sci U S A*, 2009, 106, 17235-17240.
4. M. M. Ivancic, E. L. Huttlin, X. Chen, J. K. Pleiman, A. A. Irving, A. D. Hegeman, W. F. Dove and M. R. Sussman, *J Proteome Res*, 2013, 12, 4152-4166.
5. C. Webhofer, P. Gormanns, S. Reckow, M. Lebar, G. Maccarrone, T. Ludwig, B. Putz, J. M. Asara, F. Holsboer, I. Sillaber, W. Zieglgansberger and C. W. Turck, *J Psychiatr Res*, 2013, 47, 289-298.
6. Y. Zhang, M. D. Filiou, S. Reckow, P. Gormanns, G. Maccarrone, M. S. Kessler, E. Frank, B. Hambsch, F. Holsboer, R. Landgraf and C. W. Turck, *Mol Cell Proteomics*, 2011, 10, M111.008110.
7. E. Frank, M. S. Kessler, M. D. Filiou, Y. Zhang, G. Maccarrone, S. Reckow, M. Bunck, H. Heumann, C. W. Turck, R. Landgraf and B. Hambsch, *PLoS ONE*, 2009, 4, e7821.
8. B. Arsova, H. Zauber and W. X. Schulze, *Mol Cell Proteomics*, 2012, 11, 619-628.
9. M. D. Filiou, J. Varadarajulu, L. Teplytska, S. Reckow, G. Maccarrone and C. W. Turck, *Proteomics*, 2012, 12, 3121-3128.
10. S. Kierszniowska, D. Walther and W. X. Schulze, *Proteomics*, 2009, 9, 1916-1924.
11. M. R. Russell and K. S. Lilley, *J Proteomics*, 2012, 77, 441-454.
12. B. Cox and A. Emili, *Nat Protoc*, 2006, 1, 1872-1878.
13. M. D. Filiou, B. Bisle, S. Reckow, L. Teplytska, G. Maccarrone and C. W. Turck, *Electrophoresis*, 2010, 31, 1294-1301.
14. C. Webhofer, Y. Zhang, J. Brusis, S. Reckow, R. Landgraf, G. Maccarrone, C. W. Turck and M. D. Filiou, *J Proteomics*, 2013, 88, 27-33.
15. Y. Y. Zhang, C. Webhofer, S. Reckow, M. D. Filiou, G. Maccarrone and C. W. Turck, *Proteomics*, 2009, 9, 4265-4270.
16. A. Keller, A. I. Nesvizhskii, E. Kolker and R. Aebersold, *Anal Chem*, 2002, 74, 5383-5392.
17. A. Keller, J. Eng, N. Zhang, X. J. Li and R. Aebersold, *Mol Syst Biol*, 2005, 1, 2005 0017.
18. M. J. MacCoss, C. C. Wu, D. E. Matthews and J. R. Yates, 3rd, *Anal Chem*, 2005, 77, 7646-7653.

19. C. Pan, G. Kora, W. H. McDonald, D. L. Tabb, N. C. VerBerkmoes, G. B. Hurst, D. A. Pelletier, N. F. Samatova and R. L. Hettich, *Anal Chem*, 2006, 78, 7121-7131.
20. T. Hulsen, J. de Vlieg and W. Alkema, *BMC Genomics*, 2008, 9.
21. N. L. Anderson and N. G. Anderson, *Mol Cell Proteomics*, 2002, 1, 845-867.
22. H. Liu, R. G. Sadygov and J. R. Yates, 3rd, *Anal Chem*, 2004, 76, 4193-4201.
23. D. L. Tabb, L. Vega-Montoto, P. A. Rudnick, A. M. Variyath, A. J. Ham, D. M. Bunk, L. E. Kilpatrick, D. D. Billheimer, R. K. Blackman, H. L. Cardasis, S. A. Carr, K. R. Clauser, J. D. Jaffe, K. A. Kowalski, T. A. Neubert, F. E. Regnier, B. Schilling, T. J. Tegeler, M. Wang, P. Wang, J. R. Whiteaker, L. J. Zimmerman, S. J. Fisher, B. W. Gibson, C. R. Kinsinger, M. Mesri, H. Rodriguez, S. E. Stein, P. Tempst, A. G. Paulovich, D. C. Liebler and C. Spiegelman, *J Proteome Res*, 2010, 9, 761-776.
24. P. D. Piehowski, V. A. Petyuk, D. J. Orton, F. Xie, R. J. Moore, M. Ramirez-Restrepo, A. Engel, A. P. Lieberman, R. L. Albin, D. G. Camp, R. D. Smith and A. J. Myers, *J Proteome Res*, 2013, 12, 2128-2137.
25. M. D. Filiou, C. Webhofer, P. Gormanns, Y. Zhang, S. Reckow, B. Bisle, L. Teplytska, E. Frank, M. S. Kessler, G. Maccarrone, R. Landgraf and C. W. Turck, *Proteomics*, 2012, 12, 2421-2427.

Table legends

Table 1: Identified peptides and protein groups derive from both from ^{14}N and ^{15}N-labeled mouse brain and plasma. Protein groups identified with ≥ 2 non-redundant peptides and a false discovery rate (FDR) of 1% are reported.

Table 2: Assessed characteristics of the $^{15}N/^{14}N$ workflow in plasma/brain technical replicates and plasma/brain sample preparation replicates.

Figure legends

Fig. 1: Experimental design for the assessment of variability in mouse plasma and brain specimens using the ^{15}N metabolic labeling workflow.

Fig. 2: Peptide and proteome profiling characteristics. Unique ^{14}N and ^{15}N labelled peptides identified per protein and protein sequence coverage (%) in: **A.** plasma and brain technical replicates **B.** brain sample preparation replicates.

Fig. 3: Selected ion chromatogram, full scan MS spectra of ^{14}N and ^{15}N isotope cluster of peptide signals (m/z) generated using the ProRata software and identified peptide sequence. **A.** ^{14}N and ^{15}N isotope clusters have a S/N ratio >2. **B.** ^{14}N and ^{15}N isotope clusters have a S/N ratio < 2. **C.** Overlap between two isotope clusters. ProRata software does not consider for subsequent quantification ^{14}N and ^{15}N isotope clusters which follow the case depicted in **B** and **C** panels.

Table 1

	Plasma						Brain					
	Technical replicates			Sample preparation replicates			Technical replicates			Sample preparation replicates		
Sample	1	2	3	1	2	3	1	2	3	1	2	3
Non-redundant peptides	2295	2156	2246	2295	2126	2327	8678	8751	8790	8790	6478	7563
Non-redundant protein groups	171	166	168	171	169	170	1193	1217	1205	1205	891	1034

Table 2

	Plasma		Brain	
Assessed parameter	**Technical replicates**	**Sample preparation replicates**	**Technical replicates**	**Sample preparation replicates**
R^2 (average), LC-variability RT	0.96	0.93	0.98	0.95
Identified peptides in all three replicates	1688	1353	5985	3716
% peptide overlap in all three replicates	60.26	41.39	51.04	30.68
Identified protein groups in all three replicates	140	130	961	705
% protein group overlap in all three replicates	69.65	60.75	65.46	50.18
R^2 (average) [protein $\log_2(^{15}N/^{14}N)$] Overall quantification variability	0.91	0.84	0.78	0.76

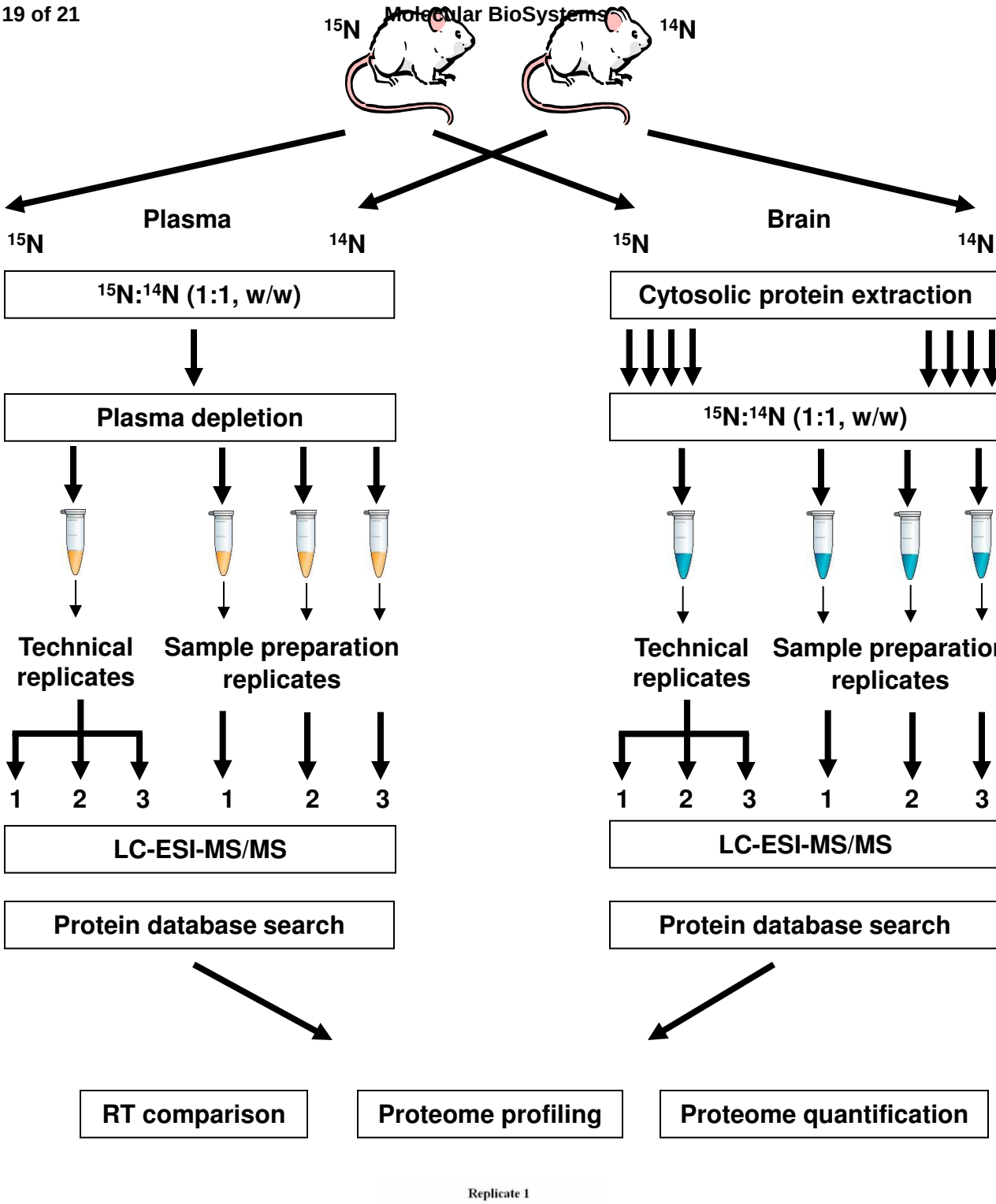

Fig 1

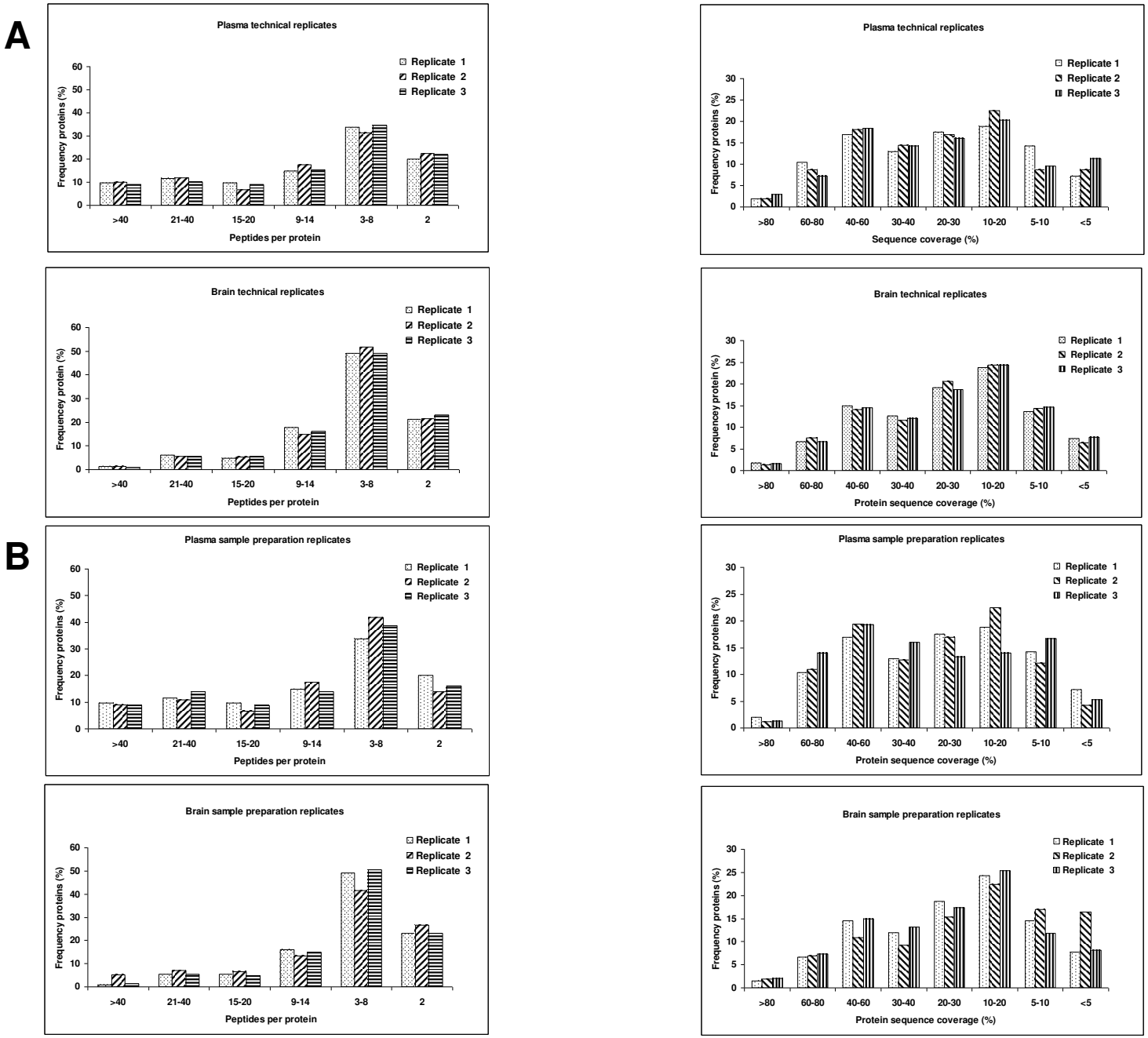

Fig 2

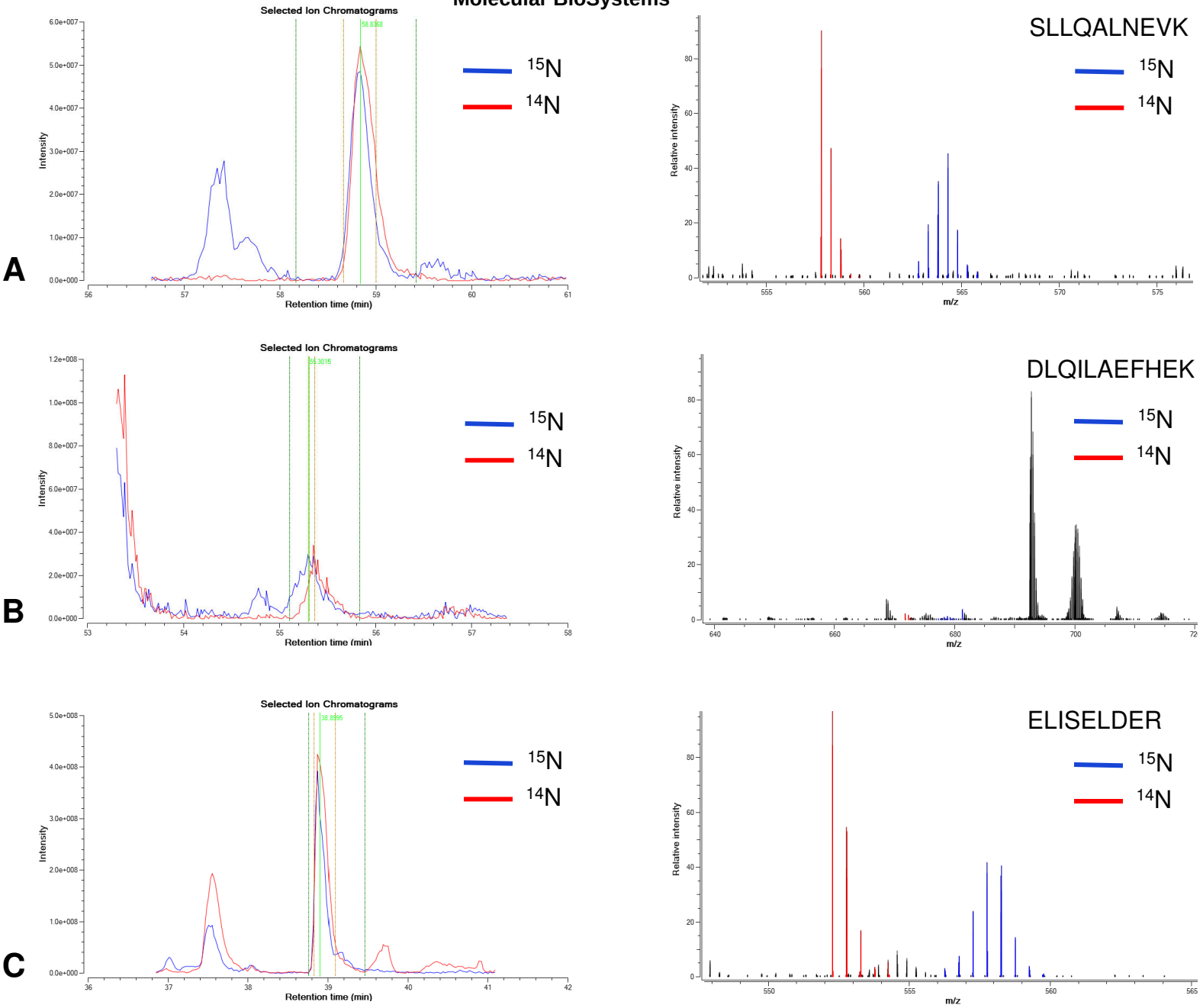

Fig. 3